

Magnetic properties of the heavy fermion antiferromagnet CeMg_3

Pranab Kumar Das, Neeraj Kumar, R. Kulkarni and A. Thamizhavel

*Department of Condensed Matter Physics and Materials Science,
Tata Institute of Fundamental Research, Homi Bhabha Road, Colaba, Mumbai 400 005, India.*

(Dated: October 25, 2018)

We have grown the single crystals of CeMg_3 and its non-magnetic analogue LaMg_3 , which crystallize in the cubic crystal structure with the space group $Fm\bar{3}m$, and studied their magnetic properties on well oriented single crystals by measuring the magnetic susceptibility, magnetization, electrical resistivity and heat capacity. CeMg_3 orders antiferromagnetically with a Néel temperature T_N of 2.6 K. The specific heat capacity at low temperature exhibits an enhanced Sommerfeld coefficient of $370 \text{ mJ/K}^2 \cdot \text{mol}$ indicating the heavy fermion nature of CeMg_3 . An estimation of Kondo temperature T_K was made and found that it is of similar magnitude as that of T_N . The reduced value of the magnetization below the ordering temperature, together with the reduced entropy at the magnetic ordering temperature and the enhanced low temperature heat capacity indicates that Kondo effect plays a significant role in this compound. The electrical resistivity measurement suggests that CeMg_3 is a Kondo lattice compound. We have performed the crystalline electric field (CEF) analysis on the magnetic susceptibility and the heat capacity data and found that the ground state is a Γ_7 doublet with an overall splitting of 191 K.

PACS numbers: 81.10.-h, 71.27.+a, 71.70.Ch, 75.10.Dg, 75.50.Ee

I. INTRODUCTION

The magnetism due to the localized $4f$ electrons in the rare-earth based intermetallic compounds is always interesting due to the wide range of physical properties exhibited by these compounds. The binary rare-earth intermetallic systems have been studied over several decades. In particular, the Ce based binary compounds are the most extensively studied as they exhibit many novel magnetic behavior owing to the close proximity of the $4f$ level to the Fermi level. Like for example, CeAl_3 and CeCu_6 are heavy fermion Kondo lattice compounds without any long-range magnetic order^{1,2}, the cubic CeAl_2 and CeB_6 are Kondo lattice compounds that order magnetically at low temperature^{3,4}. Pressure induced superconductivity is observed in the binary compound CeIn_3 ⁵. In view of these interesting properties of binary compounds, we wanted to investigate the magnetic properties of RMg_3 ($R = \text{La}$ and Ce) compounds which crystallize in the cubic BiF_3 - type structure. In one of the early reports on RMg_3 system, Buschow has studied the magnetic properties of CeMg_3 and NdMg_3 and reported no magnetic ordering, down to 4.2 K, in these two compounds⁶. However, Galera *et al* and Pierre *et al* have found that CeMg_3 orders antiferromagnetically at 3.4 K^{7,8}, while NdMg_3 orders magnetically at 6 K⁸. From the previous neutron scattering experiments on polycrystalline sample^{9,10}, it has been found that NdMg_3 undergoes an antiferromagnetic ordering at $T_N = 6$ K with the propagation vector $\mathbf{k} = (0.5, 0.5, 0.5)$ and the magnetic structure of NdMg_3 possesses ferromagnetic layers of (111) which are stacked in opposite direction leading to an antiferromagnetic alignment along the [111] axis. Recently, Tanida *et al* have performed a detailed magnetic measurements on PrMg_3 single crystal and found that PrMg_3 exhibits a nonmagnetic Γ_3 doublet ground state¹¹. In this paper,

we report on the detailed magnetic properties of single crystalline LaMg_3 and CeMg_3 by studying the magnetization, electrical resistivity and heat capacity measurements. A crystal electric field (CEF) analysis was performed on the susceptibility and heat capacity data and the energy levels thus obtained corroborates the previous neutron diffraction measurements performed on polycrystalline samples⁷.

II. EXPERIMENT

From the binary phase diagram of Ce-Mg and La-Mg by Nayeb-hasehmi and Clark¹² it was found that both CeMg_3 and LaMg_3 melt congruently at temperature close to 800 °C. Hence these compounds can be grown directly from the melt. Owing to the high vapor pressure of Mg, the single crystals were grown by Bridgman method. The stoichiometric amounts of the rare-earth metal and magnesium were taken in a point bottomed alumina crucible and sealed in a molybdenum tube. This molybdenum tube was then subsequently sealed in a quartz ampoule and loaded into a box type furnace. The furnace was then raised to 850 °C, well above the melting point of these compounds and held at this temperature for 24 hours. Then the samples were slowly cooled down to 780 °C over a period of 3 days. Bulk shiny single crystals were obtained by gently tapping on the alumina crucible and they were found to be stable in air. The crystals were then subjected to powder x-ray diffraction to check the phase purity. The orientation of the crystal was done by back reflection Laue method. The dc magnetic susceptibility and the magnetization measurements were performed in the temperature range 1.8-300 K using a superconducting quantum interference device (SQUID) and vibrating sample magnetometer (VSM). The electrical resistivity

was measured down to 1.9 K in a home made set up. The heat capacity was measured using a Quantum Design physical property measurement system (PPMS).

III. RESULTS

A. X-ray diffraction

Small pieces of the single crystals were crushed into fine powder and subjected to powder x-ray diffraction, using a PANalytical x-ray diffractometer with monochromatic Cu- K_α radiation, to check the phase purity and to estimate the lattice constant values. No traces of any secondary phases were seen in the x-ray diffractogram indicating the samples are phase pure. A Rietveld analysis was performed and the representative powder x-ray diffraction pattern of CeMg_3 is shown in Fig. 1. A reasonably good fit of the experimental pattern confirms the space group $Fm\bar{3}m$ (#225) and the estimated lattice con-

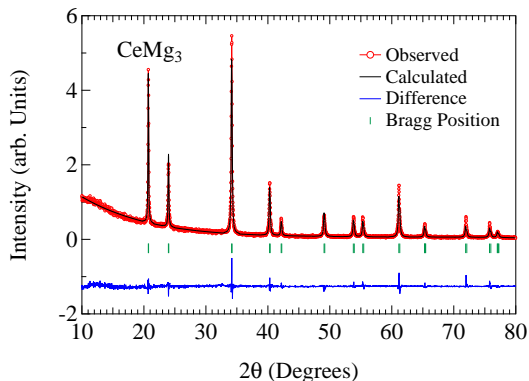


FIG. 1: (Color online) A representative powder x-ray diffraction pattern of CeMg_3 .

stant was 7.468 \AA for LaMg_3 and 7.422 \AA for CeMg_3 . It is worth mentioning here that the nearest Ce-Ce distance is 5.248 \AA . Hence, CeMg_3 is a good system to study the competing Ruderman-Kittel-Kasuya-Yosida (RKKY) interaction and Kondo screening. The stoichiometry of the samples was further confirmed by the energy dispersive analysis by x-ray (EDAX) where the composition of the single crystal was analysed at various regions of the single crystal. It was found that the sample is highly homogeneous maintaining the stoichiometry through out the sample. The crystals were then oriented along the principal crystallographic direction namely $[100]$, by means of Laue back reflection. The four fold symmetry of the Laue pattern confirmed the cubic structure of this compound. The crystals were then cut along $[100]$ by means of a spark erosion cutting machine for the magnetic property measurements.

B. Magnetization

The temperature dependence of magnetic susceptibility of CeMg_3 from 1.8 to 300 K in an applied magnetic field of 1 kOe for H parallel to $[100]$ direction is shown in Fig. 2(a). The inset shows the low temperature part of

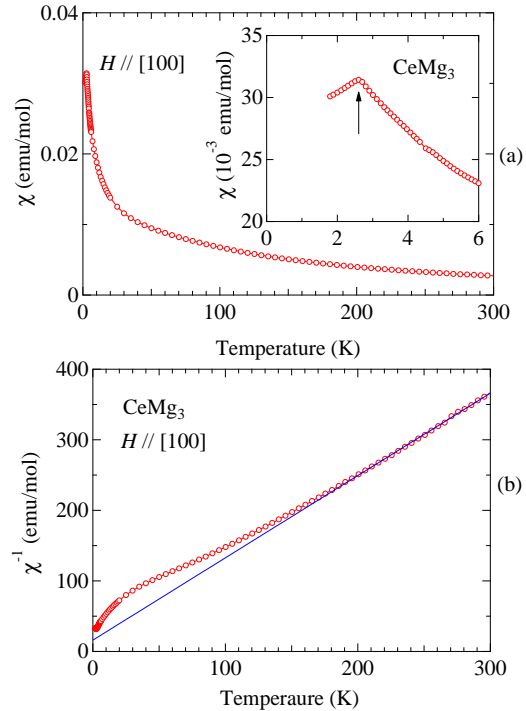


FIG. 2: (Color online) (a) Temperature dependence of magnetic susceptibility of CeMg_3 for field parallel to $[100]$. The inset shows the low temperature part of the magnetic susceptibility in an expanded scale. (b) Inverse magnetic susceptibility of CeMg_3 , the solid line is a fit to Curie-Weiss law.

the magnetic susceptibility where the susceptibility exhibits a cusp at 2.6 K and drops with the decrease in the temperature. This cusp in the magnetic susceptibility at 2.6 K is the Néel temperature of CeMg_3 where the Ce moments order antiferromagnetically. The magnetic ordering temperature at 2.6 K here is less than what it has been reported on polycrystalline sample earlier⁸. The heat capacity measurement to be discussed later confirms the bulk magnetic ordering at this temperature. Figure 2(b) shows the inverse magnetic susceptibility. At high temperature the inverse magnetic susceptibility is linear and follows Curie-Weiss law for temperature above 200 K. The solid line in Fig. 2(b) is a fit to the Curie-Weiss law. From the fitting, effective magnetic moment μ_{eff} and the paramagnetic Curie temperature θ_p were found to be $2.61 \mu_B/\text{Ce}$ and -12 K , respectively. The estimated effective moment is close to the free ion value of Ce, $2.54 \mu_B$ in its trivalent state. The negative sign of the θ_p indicates the antiferromagnetic nature of the magnetic ordering. The inverse susceptibility deviates

from the linearity for temperature less than 200 K which is mainly attributed to the crystal electric field (CEF) effect.

The field dependence of magnetization $M(H)$ at a constant temperature $T = 1.8$ K is shown in Fig. 3. The magnetization is almost linear up to a field of 12 T, thus confirming the antiferromagnetic ordering of the Ce mo-

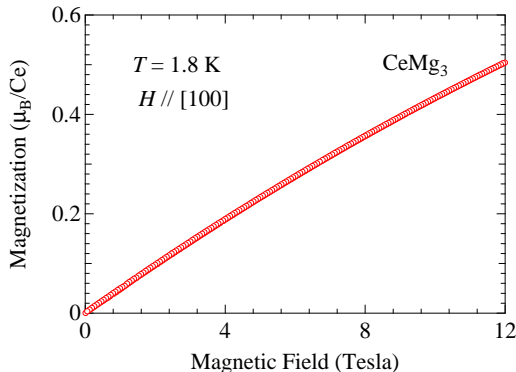


FIG. 3: (Color online) Isothermal magnetization of CeMg_3 for $H \parallel [100]$ at $T = 1.8$ K measured in a vibrating sample magnetometer.

ments. The magnetization does not show any signature of saturation up to a field of 12 T and attains a value of only $0.5 \mu_B/\text{Ce}$, thus corroborating the previous neutron diffraction experimental results where an ordered moment of $0.59 \mu_B$ is observed⁸. The saturation moment of a free Ce^{3+} ion $g_J J \mu_B$ is $2.14 \mu_B$ with $g_J = 6/7$ and $J = 5/2$. The observed magnetization is much reduced compared to the free Ce^{3+} ion and this reduction in the magnetization is attributed to the Kondo effect and CEF effect.

C. Electrical Resistivity

The electrical resistivity of CeMg_3 and LaMg_3 in the temperature range from 1.9 to 300 K, for current parallel to $[100]$ direction is shown in the main panel of Fig. 4. The antiferromagnetic ordering at 2.6 K is not clearly discernible here as the resistivity was measured down only to 1.9 K. The $\rho(T)$ of LaMg_3 decreases with the decrease in temperature, typical of a metallic compound without any anomaly at low temperature while the electrical resistivity for CeMg_3 initially decreases with decreasing temperature and exhibits a broad curvature at around 150 K followed by a minimum at 30 K. Below 30 K, the resistivity shows a weak increase and then decreases. The broad hump at 150 K may be attributed to the combined influence of the crystal field and Kondo effects. The inset shows the magnetic part of the resistivity ρ_{mag} , obtained by subtracting ρ_{LaMg_3} from ρ_{CeMg_3} , in semi-logarithmic scale. ρ_{mag} increases with the decrease in temperature below 300 K and shows two broad peaks centered around

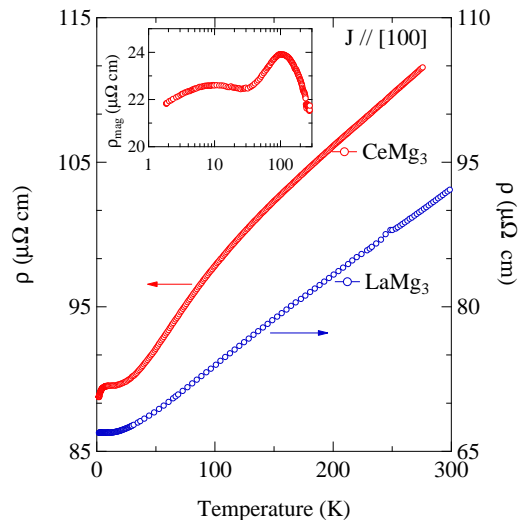


FIG. 4: (Color online) (a) Temperature dependence of electrical resistivity $\rho(T)$ of CeMg_3 and LaMg_3 in the temperature range 1.9 to 300 K. Inset shows the magnetic part of the electrical resistivity $\rho_{\text{mag}}(T)$.

6 K and 100 K. This type of double peaked structure in $\rho_{\text{mag}}(T)$ is often observed in Kondo lattice compounds, exhibiting a magnetically ordered ground states. Hence, CeMg_3 can be termed as a Kondo lattice compound. The $\rho_{\text{mag}}(T)$ varies nearly as $-\ln(T)$ at low and high temperatures. According to Cornut and Coqblin¹³, this type of behaviour is expected for Kondo type interaction in the presence of strong crystal field splitting with the Kondo temperature T_K much less than the over all crystal field splitting Δ_{CEF} . The low temperature peak in $\rho_{\text{mag}}(T)$ may be attributed to the Kondo scattering of the conduction electrons with an energy scale of the order of Kondo temperature T_K . The estimation of T_K is given in the discussion part.

D. Heat Capacity

The temperature dependence of the specific heat capacity of single crystalline CeMg_3 and LaMg_3 are shown in the main panel of Fig. 5(a). The heat capacity of LaMg_3 does not show any anomaly, and its temperature dependence is typical for a non-magnetic reference compound. The low temperature part of the heat capacity of CeMg_3 is shown in the top inset of Fig. 5(a), where a clear jump is seen at $T_N = 2.6$ K, confirming the bulk magnetic ordering in this compound. No anomaly is seen at 3.5 or 4 K as claimed by Galera et al⁸ in the earlier studies on polycrystalline samples. Thus the antiferromagnetic ordering in CeMg_3 is confirmed to be at 2.6 K. The low temperature part of the C/T vs. T^2 plot is shown in Fig. 5(a) and the magnitude of the Sommerfeld coefficient γ is obtained by fitting the expression $C/T = \gamma + \beta T^2$. The γ value thus obtained was es-

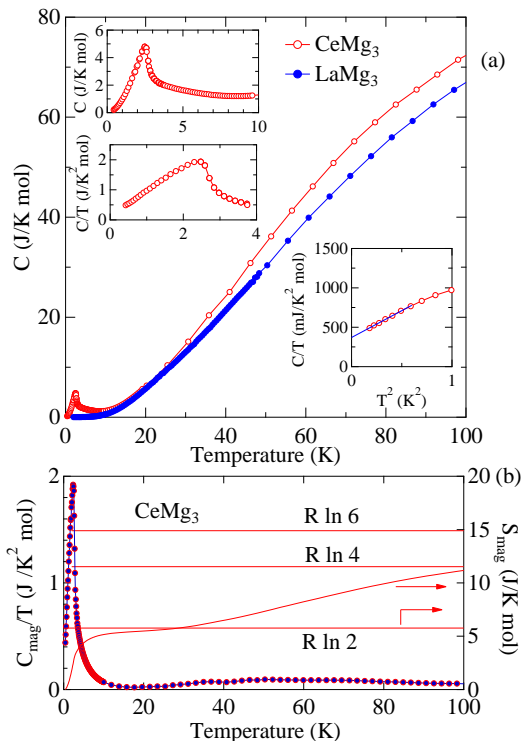


FIG. 5: (Color online) (a) Temperature dependence of the specific heat capacity in CeMg_3 and LaMg_3 . The top insets show the low temperature plots of C vs. T and C/T vs. T of CeMg_3 . The bottom inset shows the C/T vs T^2 plot. (b) C_{mag}/T vs. T of CeMg_3 . The calculated entropy is plotted in the right axis.

estimated to be $370 \text{ mJ/K}^2 \cdot \text{mol}$, and the β value is estimated to be $608 \text{ mJ/K}^4 \cdot \text{mol}$. The high temperature γ_{HT} estimated in the paramagnetic state ($12 \text{ K} < T < 17 \text{ K}$) results in a value of $41 \text{ mJ/K}^2 \cdot \text{mol}$. This implies that the enhanced low temperature γ value is due to the strong Kondo interaction. The large value of γ in the low temperature region indicates that CeMg_3 is a heavy fermion compound, while the obtained β value implies the expected contribution from the magnons, in the magnetic structure. The large value of the γ also signals the enhanced density of quasi-particle state at the Fermi level. The magnetic part of heat capacity C_{mag} was estimated by the usual method of subtracting the heat capacity of LaMg_3 from CeMg_3 . C_{mag} shows a broad peak centered around 80 K indicating the Schottky anomaly. The energy level scheme is given in the discussion part. The C_{mag}/T versus temperature plot and the calculated entropy is shown in Fig. 5(b). At T_N ($= 2.6 \text{ K}$) the entropy amounts to only $0.5R \ln 2$ with respect to the value of $R \ln 2$ anticipated for a doublet ground state. The reduced value of $R \ln 2$ further confirms the Kondo effect in CeMg_3 .

Figure 6 shows the C/T versus T plot of CeMg_3 measured in applied fields of 0, 1 and 5 T. There is no appre-

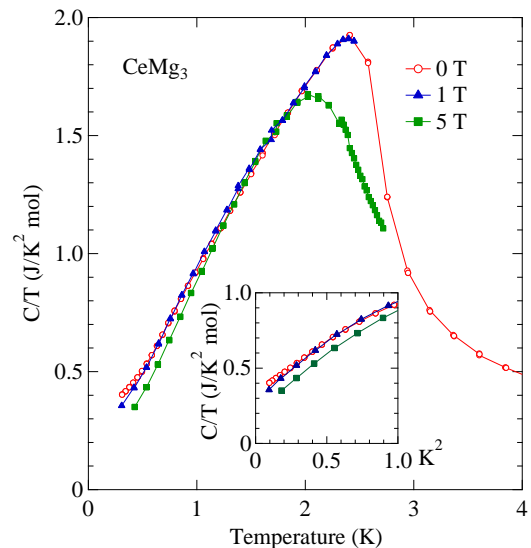


FIG. 6: (Color online) (a) C/T versus T plot of CeMg_3 in applied magnetic fields, in the temperature range 0.5 to 4 K. The inset shows the low temperature part of C/T versus T^2 plot.

ciable change in the ordering temperature in an applied field of 1 T while in a 5 T field, the Néel temperature shifts to lower temperature and the jump in the heat capacity also decreases as it is usually observed in antiferromagnetically ordering compounds. The low temperature part of C/T versus T^2 plot is shown in the inset of Fig. 6. An estimation of the γ value by linear extrapolation of the C/T versus T^2 plot of the heat capacity data measured in 1 T and 5 T field results in 300 and 200 $\text{mJ/K}^2 \cdot \text{mol}$, respectively. The reduction in the γ value implies that the application of magnetic field tends to break the Kondo coupling between the localized $4f$ electron and the conduction electrons.

IV. DISCUSSION

The previous studies on polycrystalline samples of CeMg_3 have claimed that this compound orders antiferromagnetically at 4 K ⁸. However, it is ubiquitous from our magnetic and thermal measurements on clean phase pure single crystals that CeMg_3 orders antiferromagnetically at 2.6 K . The large value of the Sommerfeld coefficient γ at low temperature indicates enhanced density of states at the Fermi level which is due to the result of Kondo effect. The electrical resistivity measurement clearly indicates that CeMg_3 is a Kondo lattice compound. The reduced value of the magnetic moment of $0.5 \mu_B/\text{Ce}$ at $T = 1.8 \text{ K}$ in a field of 12 T and a very small heat capacity jump at the magnetic ordering temperature further confirms the Kondo effect in CeMg_3 . We made an estimate of the Kondo Temperature T_K by the method described by Bredl *et al.*¹⁴, where in the mean

field approach, the jump in the heat capacity ΔC_{mag} of a Kondo system is related to the Kondo temperature. Besnus *et al*¹⁵ have found that the estimation of T_K by this model agrees well with the experimental data on various Ce and Yb compounds. From Eqs. (12), (13) and (15) of Ref. 14, Blanco *et al.* have given the expression for ΔC_{mag} at the magnetic ordering temperature as,

$$\Delta C_{\text{mag}} = \frac{6N_A k_B}{\psi''' \left(\frac{1}{2} + x\right)} \left[\psi' \left(\frac{1}{2} + x\right) + x\psi'' \left(\frac{1}{2} + x\right) \right]^2, \quad (1)$$

where $x = (T_K/T_N)/2\pi$ and ψ' , ψ'' and ψ''' are the first, second and third derivative of the polygamma function and the other terms have the usual meaning. A plot of this function is shown in Fig 7. The jump in the magnetic part of the heat capacity was estimated to be 4.35 J/K · mol, which results in a T_K value of 3.5 K. Desgranges and Schotte¹⁷ have theoretically explained that

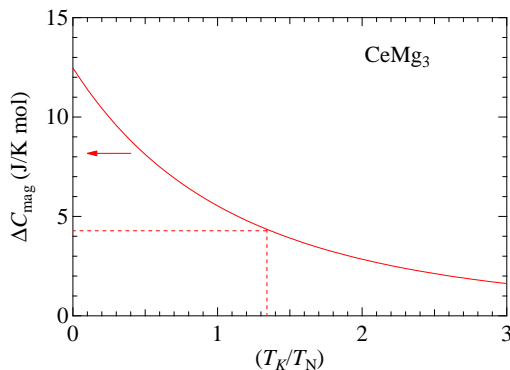


FIG. 7: (Color online) Estimation of the Kondo temperature from the jump in the magnetic part of the heat capacity. The solid line is the plot of Eq. 1. See text for details.

the entropy of a Kondo system at the characteristic temperature T_K amounts to $0.68 R \ln 2$ ($= 3.92$ J/K · mol). According to this expression, for CeMg_3 , $0.68 R \ln 2$ is reached at 3.8 K which indicates that this Kondo temperature is in close agreement with the one estimated from Eq. 1. Furthermore, the Kondo temperature can also be estimated from the paramagnetic Curie-Weiss temperature as mentioned by Gruner *et al*¹⁸, $|\theta_p|/4$ ($12/4 = 3$ K). The estimation of Kondo temperature T_K by various methods gives a value of 3-4 K, which is close to the magnetic ordering temperature of CeMg_3 . However, a detailed neutron diffraction experiment has to be performed to substantiate our estimation of T_K .

The magnetic part of the heat capacity C_{mag} of CeMg_3 shows a broad peak at high temperature as shown in Fig. 8(a). This feature is attributed to the Schottky excitations between the CEF levels of the Ce^{3+} ions. We have performed an analysis of the heat capacity and the magnetic susceptibility data on the basis of CEF model. The Schottky contribution to heat capacity is given by the following expression,

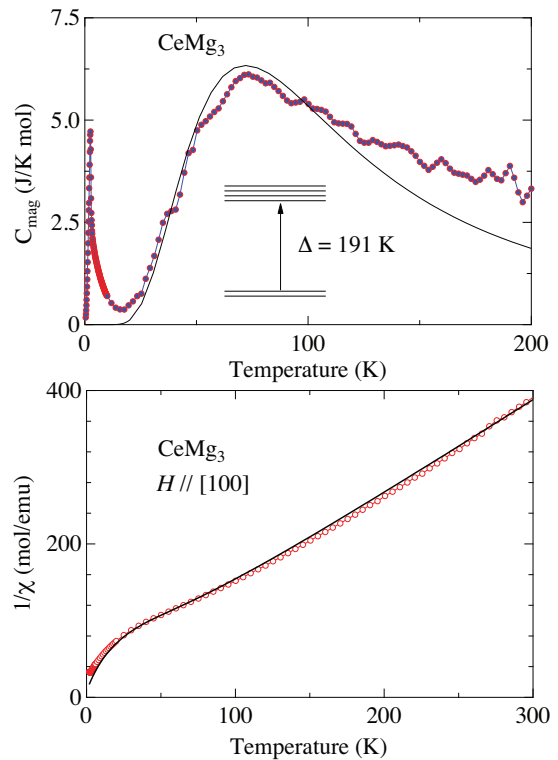


FIG. 8: (Color online) (a) Magnetic part of the specific heat capacity of CeMg_3 . The solid line is calculated Schottky heat capacity, which gives an energy separation of 191 K between the ground state doublet and the excited quartet. (b) Inverse magnetic susceptibility of CeMg_3 . The solid line is based on the CEF calculation.

$$C_{Sch}(T) = R \frac{\left[\sum_i g_i e^{-E_i/T} \sum_i g_i E_i^2 e^{-E_i/T} - \left[\sum_i g_i E_i e^{-E_i/T} \right]^2 \right]}{T^2 \left[\sum_i g_i e^{-E_i/T} \right]^2} \quad (2)$$

where R is the gas constant, E_i is the CEF energy level in units of temperature and g_i the corresponding degeneracy. The Ce atom in CeMg_3 possesses a cubic site symmetry and hence the ground state should be a doublet or quartet. From the entropy calculations discussed above, it is obvious that the ground state of CeMg_3 should be a doublet ground state. Considering a degeneracy of doublet ground state and a quartet excited state, we found that the CEF levels are separated by an energy of 191 K apart. The solid line in Fig. 8(a) indicates the calculated Schottky heat capacity which is matching well with the experimental data.

The crystalline electric field analysis was also performed on the magnetic susceptibility data. For a cubic point symmetry, the CEF Hamiltonian is given by,

$$\mathcal{H}_{\text{CEF}} = B_4^0 (O_4^0 + 5O_4^4) + B_6^0 (O_6^0 - 21O_6^4) \quad (3)$$

, where B_l^m and O_l^m are the crystal field parameters and

the Steven's operators respectively^{19,20}. For Ce atom, the sixth order terms O_6^0 and O_6^4 vanish and hence the CEF Hamiltonian reduces to

$$\mathcal{H}_{\text{CEF}} = B_4^0 (O_4^0 + 5O_4^4) \quad (4)$$

The CEF susceptibility is given by the expression,

$$\chi_{\text{CEF}i} = N(g_J\mu_B)^2 \frac{1}{Z} \left(\sum_{m \neq n} |\langle m | J_i | n \rangle|^2 \frac{1 - e^{-\beta\Delta_{m,n}}}{\Delta_{m,n}} e^{-\beta E_n} + \sum_n |\langle n | J_i | n \rangle|^2 \beta e^{-\beta E_n} \right), \quad (5)$$

where g_J is the Landé g -factor, E_n and $|n\rangle$ are the n th eigenvalue and eigenfunction, respectively. J_i ($i = x, y$ and z) is a component of the angular momentum, and $\Delta_{m,n} = E_n - E_m$, $Z = \sum_n e^{-\beta E_n}$ and $\beta = 1/k_B T$. The magnetic susceptibility including the molecular field contribution λ_i is given by

$$\chi_i^{-1} = \chi_{\text{CEF}i}^{-1} - \lambda_i. \quad (6)$$

The CEF parameter B_4^0 was estimated by using the Eqns. 4, 5 and 6. The solid line Fig. 8(b) is the calculated CEF curve and the value of B_4^0 thus obtained is 0.53 K and the molecular field contribution λ was -8 mol/emu. The sign of the B_4^0 parameter is positive, which clearly indicates that the ground state is a Γ_7 doublet. From the eigen values of the crystal field Hamiltonian the crystal field splitting energy was found to be 191 K. The crystal field level scheme thus obtained from the magnetic susceptibility and the heat capacity data are in accordance with the previous neutron diffraction results on polycrystalline samples^{7,9}. The magnitude of the ordered moment of a Γ_7 doublet ground state based on the CEF calculation ($g_J J_x = 6/7 \times 0.833$) should be $0.714 \mu_B/\text{Ce}$. The observed magnetization value at 1.8 K is only $0.56 \mu_B/\text{Ce}$, this confirms that the moment reduction in this compound is due to the combined effect of Kondo and crystal field effects.

The overall magnetic behaviour of CeMg_3 resembles to that of the popular antiferromagnetically ordered heavy fermion systems like CeIn_3 ²¹, CePd_2Si_2 ⁵ and CeCu_2Ge_2 ²². These systems have their Néel and Kondo temperatures nearly equal and exhibit pressure induced superconductivity. The ordered moment in these compounds are also considerably reduced, and these compounds also possess enhanced Sommerfeld coefficient γ ,

as it has been observed in the present CeMg_3 system. All these implies that CeMg_3 is another compound where the high pressure studies will yield some interesting results.

V. CONCLUSION

Single crystals of LaMg_3 and CeMg_3 were grown by Bridgman method in sealed molybdenum tubes. X-ray and EDAX analysis of the sample confirmed the stoichiometry of the single crystals. The magnetic susceptibility and the heat capacity clearly indicated the antiferromagnetic ordering at $T_N = 2.6$ K. The heavy fermion nature of this compound is confirmed by the large Sommerfeld coefficient $\gamma = 370$ mJ/K² · mol. The reduced value of the magnetization and the reduced magnetic entropy at the magnetic ordering temperature and the $-\ln(T)$ behaviour in the electrical resistivity confirmed the significant contribution of the Kondo effect in CeMg_3 . The estimated Kondo temperature T_K was found to be 3-4 K which is close to the magnetic ordering temperature, suggesting a delicate competition between the Kondo effect and the indirect exchange interaction. Since the T_N and T_K are very close in CeMg_3 , it will be interesting to study the effect of pressure on the electrical resistivity of CeMg_3 , which is planned for the future. The CEF analysis of the heat capacity and the magnetic susceptibility data indicated that the ground state is a Γ_7 doublet while the excited state is a Γ_8 quartet with an energy splitting of 191 K.

VI. ACKNOWLEDGEMENT

The discussions with Prof. S. K. Dhar is gratefully acknowledged.

¹ K. Andres, J. E. Graebner and H. R. Ott, Phys. Rev. Lett **35**, 1779 (1975).

² Y. Ōnuki, Y. Shimizu and T. Komatsubara, J. Phys. Soc. Japan **53**, 1210 (1984).

³ B. Barbara, J. X. Boucherle et al., Solid State Commun. **24**, 481 (1977).

⁴ K. Winzer, Solid State Commun. **16**, 521 (1975).

⁵ F. M. Grosche, I. R. Walker, S. R. Julian, N. D. Mathur,

- D. M. Freye, M. J. Steiner and G. G. Lonzarich, *J. Phys. Condens. Matter* **13**, 2845 (2001).
- ⁶ K.H.J. Buschow, *J. Less Comm. Metals* **44**, 301 (1976).
- ⁷ J. Pierre, A. P. Murani and R.M. Galera, *J. Phys. F: Met. Phys.* **11**, 679 (1981).
- ⁸ R. M. Galera, J. Pierre and J. Pannetier, *J. Phys. F: Met. Phys.*, **12**, 993 (1982).
- ⁹ R. M. Galera, A. P. Murani and J. Pierre, *J. Magn. Magn. Materials*, **23** 317, (1981).
- ¹⁰ T. Chatterji, G. J. Schneider and R. M. Galera, *Phys. Rev. B*, **78**, 012411 (2008).
- ¹¹ H. Tanida, H. S. Suzuki, S. Takagi, H. Onodera and K. Tanigaki, *J. Phys. Soc. Jpn.* **75**, 073705 (2006).
- ¹² B. Nayeb-hashemi and J. Clark, *Bull. Alloy Phase Diagrams*, **9**, 916 (1988).
- ¹³ B. Cornut and B. Coqblin *Phys. Rev. B* **5**, 4541 (1972).
- ¹⁴ C. D. Bredl, F. Stglich and K. D. Schotte, *Z. Phys. B* **29**, 327 (1978).
- ¹⁵ M. J. Besnus, A. Braghta, N. Hamdaoui and A. Meyer, *J. Magn. Magn. Mater.* , **104-107**, 1385 (1992).
- ¹⁶ J. A. Blanco, M. de Podesta, J. I. Espeso, J. C. Gómez Sal, C. Lester, K. A. McEwen, N. Patrikios, J. Rodríguez Fernández, *Phys. Rev. B*, **49**, 15126 (1994).
- ¹⁷ H.-U. Desgranges and K. D. Schotte, *Phys. Lett.* **91A**, 240 (1982).
- ¹⁸ G. Grüner and A. Zawadowski, *Rep. Prog. Phys.* **37**, 1497 (1974).
- ¹⁹ K. W. H. Stevens, *Proc. Phys. Soc., London, Sect. A* **65**, 209 (1952).
- ²⁰ M. T. Hutchings, in *Solid State Physics: Advances in Research and Applications*, edited by F. Seitz and B. Turnbull (Academic, New York, 1965), Vol.16, p.227.
- ²¹ G. Knebel, D. Braithwaite, P. C. Canfield, G. Lapertot and J. Flouquet, *Phys. Rev. B* **65**, 024425 (2001).
- ²² D. Jaccard, K. Behnia and J. Sierro, *Phys. Lett. A* **163**, 475 (1992).